15 October 1998

PHYSICS LETTERS B

ELSEVIER

Physics Letters B 438 (1998) 217–228

Instanton-induced cross-sections in deep-inelastic scattering

A. Ringwald, F. Schrempp

Deutsches Elektronen-Synchrotron DESY, Hamburg, Germany

Received 3 July 1998
Editor: P.V. Landshoff

Abstract

We present our results for inclusive instanton-induced cross-sections in deep-inelastic scattering, paying in particular attention to the residual renormalization-scale dependencies. A ''fiducial'' kinematical region in the relevant Bjorken variables is extracted from recent lattice simulations of QCD. The integrated instanton-contribution to the cross-section at HERA corresponding to this fiducial region is surprisingly large: It is in the $\mathcal{O}(100)$ pb range, and thus remarkably close to the recently published experimental upper bounds.

PACS: 11.15.Kc; 12.38.Lg; 13.60.Hb
Keywords: Instanton; Chirality violation; Deep-inelastic scattering; Cross-section

1. Instantons [1] are non-perturbative gauge field fluctuations. They describe *tunnelling* transitions between degenerate vacua of *different topology* in non-abelian gauge theories like QCD. Correspondingly, instantons and anti-instantons carry an *integer topologigal* charge $Q = 1$ and $Q = -1$, respectively, while the usual perturbation theory resides in the sector $Q = 0$. Unlike the latter, instantons induce processes which violate *chirality* (Q_5) in (massless) QCD, in accord [2] with the general chiral-anomaly relation. An experimental discovery of instanton-induced events would clearly be of basic significance.

The deep-inelastic regime is distinguished by the fact that here hard instanton-induced processes may both be *calculated* [3,4] within instanton-perturbation theory and possibly *detected experimentally* [5–8]. As a key feature it has recently been shown [4], that in deep-inelastic scattering (DIS) the generic hard scale $\mathcal{Q}$ cuts off instantons with *large size* $\rho \gg \mathcal{Q}^{-1}$, over which one has no control theoretically.

In continuation of Ref. [4], where the amplitudes and cross-sections of *exclusive* partonic subprocesses relevant for DIS were calculated, we summarize in the present letter the results of our finalized calculations of the various *inclusive* instanton-induced cross-sections (Sections 2 and 4). A detailed account of our calculations will be published elsewhere [9]. The essential new aspect as compared to our first estimates [7] is the strong reduction of the residual dependence on the renormalization scale resulting from a recalculation based on an improved instanton density [10], which is renormalization-group invariant at the two-loop level.

0370-2693/98/$ - see front matter
PII: S0370-2693(98)00953-8

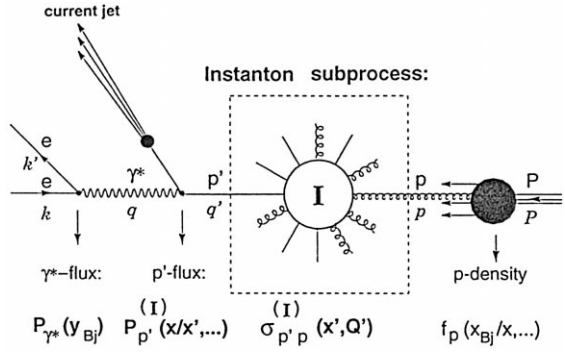

Fig. 1. The leading instanton-induced process in the DIS regime of $e^{\pm}P$ scattering.

There has been much recent activity in the lattice community to ''measure'' topological fluctuations in lattice simulations [11] of QCD. Being independent of perturbation theory, such simulations provide ''snapshots'' of the QCD vacuum including all possible non-perturbative features like instantons. They also provide crucial support for important prerequisites of our calculations in DIS, like the validity of instanton-perturbation theory and the dilute instanton-gas approximation for *small* instantons of size $\rho \leq \mathcal{O}(0.3)$ fm. As a second main point of this letter (Section 3), these lattice constraints will be exploited and translated into a ''fiducial'' kinematical region for our predictions of the instanton-induced DIS cross-section based on instanton-perturbation theory.

2. The leading instanton (I)-induced process in the DIS regime of $e^{\pm}P$ scattering for large photon virtuality Q^2 is illustrated in Fig. 1. The dashed box emphasizes the so-called instanton-*subprocess* with its own Bjorken variables,

$$Q'^2 = -q'^2 \geq 0; \quad x' = \frac{Q'^2}{2\,p\cdot q'} \leq 1. \tag{1}$$

As can be inferred from Ref. [7] and will be detailed in Ref. [9], the inclusive I-induced cross-section [1] in unpolarized deep-inelastic $e^{\pm}P$ scattering can be expressed (in the Bjorken limit) as

$$\frac{d\sigma_{eP}^{(I)}}{dx'\,dQ'^2} \simeq \sum_{p',p} \frac{d\mathscr{L}_{p'p}^{(I)}}{dx'\,dQ'^2}\,\sigma_{p'p}^{(I)}\left(x',Q'^2\right), \tag{2}$$

where $p' = q', \bar{q}'$ denotes the virtual (anti-)quarks entering the I-subprocess from the photon side and $p = q, \bar{q}, g$ denotes the target partons (c.f. Fig. 1). The differential luminosity $d\mathscr{L}_{p'p}^{(I)}$, accounting for the number of $p'p$ collisions per eP collision, has a convolution-like structure [5], involving $\{x_{\mathrm{Bj}}, y_{\mathrm{Bj}}, x\}$-integrations over the target-parton density, $f_p(x_{\mathrm{Bj}}/x,\ldots)$, the γ^*-flux, $P_{\gamma^*}(y_{\mathrm{Bj}})$, and the *known* [7,9] flux $P_{p'}^{(I)}(x/x',\ldots)$ of the parton p' in the I-background. We shall display the explicit form of the differential luminosity in Section 4.

The simple relation (2) between $d\sigma_{eP}$ and $\sigma_{p'p}^{(I)}$, derived within I-perturbation theory [7,9] in the Bjorken limit, is actually much less obvious than an inspection of the grossly oversimplified Fig. 1 may suggest. The derivation proceeds in two steps: *i*) Using the Feynman rules of I-perturbation theory in momentum space, one

[1] A sum over I-induced ($\triangle Q_5 = 2n_f$) and anti-instanton ($\bar{I}$)-induced ($\triangle Q_5 = -2n_f$) processes is always implied by the superscript (I) at cross-sections.

calculates the (manifestly gauge invariant) inclusive eP cross-section, with the current quark being not a free parton, but rather described by the (complicated) quark propagator in the I-background as in Ref. [4]. *ii*) One independently writes down the (gauge invariant) expression for the total cross-section $\sigma^{(I)}_{p'p}$ with an *off-shell* external parton p'. In the Bjorken limit, when certain non-planar contributions may be neglected, one then finds by comparison of *i*) and *ii*) the form (2) of the inclusive I-induced eP cross-section along with the explicit expression for the flux-factor $P^{(I)}_{p'}$.

While a more detailed description of this rather involved calculation has to be deferred elsewhere [9], let us summarize next the state of the art evaluation of the I-subprocess total cross-section $\sigma^{(I)}_{p'p}(x',Q'^2)$, which contains most of the crucial instanton-dynamics.

We start with the I-subprocess total cross-sections (here only for the dominating case of a target gluon) in a form [7,9] still exhibiting the complicated integrations over collective coordinates [2] (I-sizes $\rho,\bar\rho,\ldots$),

$$\sigma^{(I)}_{p'g}\simeq\int_0^\infty d\rho\int_0^\infty d\bar\rho\int d^4R\,D(\rho;\mu_r)\,D(\bar\rho;\mu_r)\left(\rho\bar\rho\mu_r^2\right)^{\beta_0\Delta_1\,\Omega\left(\frac{R2}{\rho\bar\rho},\frac{\bar\rho}{\rho}\right)}K_1(Q'\rho)\,K_1(Q'\bar\rho)$$

$$\times\exp\left[\mathrm{i}(p+q')\cdot R\right]\exp\left[-\frac{4\pi}{\alpha_s(\mu_r)}\,\Omega\left(\frac{R^2}{\rho\bar\rho},\frac{\bar\rho}{\rho}\right)\right]\frac{1}{9\sqrt{\pi}}\left(\frac{\alpha_s(\mu_r)}{4\pi}\,\frac{6}{\tilde\Omega\left(\frac{R^2}{\rho\bar\rho},\frac{\bar\rho}{\rho}\right)}\right)^{7/2}$$

$$\times(\rho\bar\rho)^{9/2}\left[\omega\left(\frac{R^2}{\rho\bar\rho},\frac{\bar\rho}{\rho}\right)\right]^{2n_f-1}\frac{2}{3}\,\frac{\pi^5}{\alpha_s(\mu_r)}\,\frac{Q'^4(p\cdot q')}{\left((p+q')^2\right)^{3/2}}\,, \tag{3}$$

where $p'=q',\bar q'$. The most important quantities entering Eq. (3) are:

- *The I-density $D(\rho,\mu_r)$,* which has the general form [2,12]

$$D(\rho,\mu_r)=d\left(\frac{2\pi}{\alpha_s(\mu_r)}\right)^6\exp\left(-\frac{2\pi}{\alpha_s(\mu_r)}\right)\frac{(\rho\mu_r)^{\beta_0\Delta_1-\Delta_2}}{\rho^5}, \tag{4}$$

with μ_r denoting the renormalization scale and [10]

$$\Delta_1\equiv 1+\frac{\beta_1}{\beta_0}\,\frac{\alpha_s(\mu_r)}{4\pi};\quad \Delta_2\equiv 12\,\beta_0\frac{\alpha_s(\mu_r)}{4\pi}, \tag{5}$$

in terms of the QCD β-function coefficients, $\beta_0=11-\frac{2}{3}n_f$; $\beta_1=102-\frac{38}{3}n_f$. The power $\beta_0\Delta_1-\Delta_2$ makes the I-density renormalization-group invariant at the two-loop level [10], $(1/D)\mathrm{d}D/\mathrm{d}\mu_r=\mathscr{O}(\alpha_s^2)$, in contrast to the original one-loop expression [2], corresponding to $\Delta_1=1$ and $\Delta_2=0$, with $(1/D)\mathrm{d}D/\mathrm{d}\mu_r=\mathscr{O}(\alpha_s)$. The constant d is scheme-dependent; in the $\overline{\mathrm{MS}}$-scheme it is given by [13] $d=C_1\exp[-3C_2+n_f C_3]/2$, with $C_1=0.46628$, $C_2=1.51137$, and $C_3=0.29175$.

[2] For brevity, we display the cross-section (3) already after the (saddle-point) integration over the I-colour orientations. The function $\tilde\Omega$, whose explicit form will be specified below, accounts for that.

Note that the large, positive power of ρ in the I-density (4) would make the integrations over the I-sizes in Eq. (3) infrared divergent without

- *the form factors $K_1(Q'\rho(\bar{\rho}))$:* For large $Q'\rho(\bar{\rho})$, the virtuality Q' of the internal quark p' in Fig. 1 provides an exponential cut-off, $K_1(Q'\rho) \propto \exp(-Q'\rho)$, in the integrations over the I-sizes [4]. These form factors where shown to arise naturally in step *i)* above, which is manifestly gauge invariant [4]. In step *ii)* one has to adopt a gauge-invariant definition of the $p'p$ cross-section, since the incoming parton p' is *off-shell* [14]. Then one obtains exactly the Bessel-K form factors [9], unlike naive, not manifestly gauge-invariant definitions which lead in addition to these well-defined contributions to unphysical ones suffering from infrared divergent I-size integrations [15,16].
- *The functions Ω and ω* (along with the integration over R_μ) summarize the effects of final-state gluons (Ω) and final-state quarks (ω). The function Ω, appearing in the exponent with a large numerical coefficient, $4\pi/\alpha_s$, and ω, occurring with a high power, $2n_f - 1$, call for a precise evaluation. Hence, let us turn next to describing their state-of-the-art evaluation.

It is very instructive to consider two alternative interpretations of the functions Ω, ω, and the integration variable R_μ.

- *Total cross-section via summation of exclusive cross-sections:*
  This is the cleanest and most straightforward method to arrive at the total cross-section. In this case one starts with the familiar representation of the $\delta^{(4)}$-function associated with energy-momentum conservation,

$$(2\pi)^4\,\delta^{(4)}\Big(p+q'-\sum_i k_i\Big)=\int d^4R\exp\left[\mathrm{i}\Big(p+q'-\sum_i k_i\Big)\cdot R\right]. \tag{6}$$

The phase-space integration over the final-state gluons/quarks is then performed by means of the basic formula

$$\int\frac{d^4k_i}{(2\pi)^3}\,\delta^{(+)}\big(k_i^2\big)\exp\big[-\mathrm{i}\,k_i\cdot R\big]=\frac{1}{(2\pi)^2}\,\frac{1}{-R^2+\mathrm{i}\epsilon R_0}, \tag{7}$$

with the help of which one finds [17]

$$\Omega\left(\frac{R^2}{\rho\bar{\rho}},\frac{\bar{\rho}}{\rho}\right)=-6\left(\frac{\rho\bar{\rho}}{-R^2+\mathrm{i}\epsilon R_0}\right)^2+12\left(\frac{\rho\bar{\rho}}{-R^2+\mathrm{i}\epsilon R_0}\right)^3\left(\frac{\rho}{\bar{\rho}}+\frac{\bar{\rho}}{\rho}\right)+\ldots \tag{8}$$

$$\omega\left(\frac{R^2}{\rho\bar{\rho}},\frac{\bar{\rho}}{\rho}\right)=4\left(\frac{\rho\bar{\rho}}{-R^2+\mathrm{i}\epsilon R_0}\right)^{3/2}+\ldots. \tag{9}$$

The interpretation of the various terms contributing to the perturbative expansion of Ω in Eq. (8) is illustrated in Fig. 2 (left): The first term takes into account the summation and exponentiation of the leading-order gluon emission, whereas the second term originates from the summation and exponentiation of interference terms between the leading-order gluon emission and the gluon-propagator correction. The first term contributing to the perturbative expansion of ω in Eq. (9) just corresponds to the leading-order quark emission.

In summary, the perturbative approach based on the exclusive amplitudes, as calculated within I-perturbation theory, yields the essential functions Ω and ω as asymptotic expansions for small $\rho\bar{\rho}/R^2$. Since ρ and $\bar{\rho}$

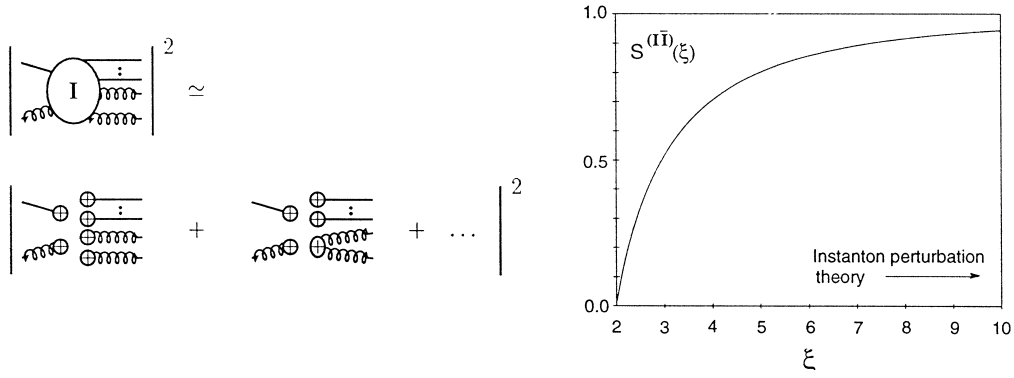

Fig. 2. *Left:* Graphical interpretation of an exclusive I-induced $q'g$ cross-section in terms of perturbation theory in the I-background. (Curly) lines ending at blobs denote LSZ-amputated quark zero modes (classical I-gauge fields). Curly lines connected by an ellipse denote LSZ-amputated gauge-field propagators in the I-background. *Right:* The $I\bar{I}$-valley action corresponding to the most attractive $I\bar{I}$-colour orientation.

are conjugate to the virtuality Q' and R is conjugate to the total momentum of the I-subprocess, $p+q'$, (c.f. Eq. (3) and Fig. 1), we expect qualitatively

$$\rho \sim \bar{\rho} \sim 1/Q' \text{ and } R^2 \sim 1/(p+q')^2 \Rightarrow \rho\bar{\rho}/R^2 \sim (p+q')^2/Q'^2 = 1/x' - 1. \tag{10}$$

Thus, strict I-perturbation theory for the total cross-section is only applicable for not too small x'.

- *Total cross-section via optical theorem and $I\bar{I}$-valley method:*

In this approach, one evaluates [18] the total cross-section from the imaginary part of the forward elastic scattering amplitude induced by the instanton-anti-instanton ($I\bar{I}$)-valley background, $A_\mu^{(I\bar{I})}$. In this case, R_μ stands for the *separation* between I and $\bar{I}$, and Ω is identified with the *interaction* between I and $\bar{I}$,

$$\Omega \simeq S^{(I\bar{I})}(\xi) - 1. \tag{11}$$

In the valley approximation, the $I\bar{I}$-valley action, $S^{(I\bar{I})} \equiv \frac{\alpha_s}{4\pi} S[A_\mu^{(I\bar{I})}]$, is restricted by conformal invariance to depend only on the ''conformal separation'' [19]

$$\xi \equiv \frac{-R^2 + i\epsilon R_0}{\rho\bar{\rho}} + \frac{\rho}{\bar{\rho}} + \frac{\bar{\rho}}{\rho}, \tag{12}$$

and its functional form is explicitly known [15,20] (Fig. 2 (right)).

Note that for all separations ξ, the interaction between I and $\bar{I}$ is *attractive* (c.f. Fig. 2 (right)): The $I\bar{I}$-valley corresponds to a configuration of steepest descent interpolating between an infinitely separated $I/\bar{I}$ pair and a strongly overlapping one, annihilating to the perturbative vacuum.

Analogously, the function ω is now identified with the *fermionic overlap integral* for which an integral representation was found in Ref. [21], which we were able to perform analytically,

$$\omega(\xi) = \frac{6B\left(\frac{3}{2},\frac{5}{2}\right)}{z^{3/2}}\, {}_2F_1\left(\frac{3}{2},\frac{3}{2};4;1-\frac{1}{z^2}\right); \quad z \equiv \frac{1}{2}\left(\xi + \sqrt{\xi^2-4}\right). \tag{13}$$

Finally, the function $\tilde{\Omega}$ arising from the integration over the relative $I\bar{I}$-colour orientations has been estimated in Ref. [16] by assuming for simplicity an orientation dependence of the valley action [3] corresponding to a dipole-dipole interaction [22],

$$\tilde{\Omega}(\xi) \simeq \xi \frac{d\Omega(\xi)}{d\xi}. \tag{14}$$

The *leading terms* in the asymptotic expansions of the $I\bar{I}$-interaction (11) and the fermionic overlap (13) for large conformal separation,

$$\Omega(\xi) = -\frac{6}{\xi^2} + \mathscr{O}\big(\ln(\xi)/\xi^4\big), \quad \omega(\xi) = \frac{4}{\xi^{3/2}} + \mathscr{O}\big(\ln(\xi)/\xi^{7/2}\big), \tag{15}$$

exactly reproduce the known perturbative results (8) and (9) for small $\rho\bar{\rho}/R^2$. This illustrates the power of the $I\bar{I}$-valley method to effectively sum up the gluonic *final-state* tree-graph corrections to the leading semi-classical result [4] [17].

We shall thus take the valley expressions for Ω, ω and $\tilde{\Omega}$, Eqs. (11), (13) and (14), to smoothly extrapolate somewhat beyond strict I-perturbation theory.

Let us add, however, that the full content of the valley approximation is not essential in this context. It is mostly the shift in the expansion variable

$$\frac{\rho\bar{\rho}}{-R^2 + i\epsilon R_0} \Rightarrow \frac{\rho\bar{\rho}}{-R^2 + i\epsilon R_0 + \rho^2 + \bar{\rho}^2} \equiv \frac{1}{\xi} \tag{16}$$

making the leading terms (15) qualitatively adequate down to fairly small $\xi(\gtrsim 3)$, in contrast to the strict I-perturbative expansions (8) and (9).

The collective coordinate integration in the cross-section (3) is perfectly suited for a *saddle-point evaluation.* To this end, we collect the most-relevant factors in Eq. (3) in the following effective exponent,

$$-\Gamma \equiv i(p+q')\cdot R - Q'(\rho+\bar{\rho}) - \left(\frac{4\pi}{\alpha_s(\mu_r)} - \Delta_1\,\beta_0 \ln\big(\rho\bar{\rho}\mu_r^2\big)\right) S^{(I\bar{I})}(\xi) - \Delta_2 \ln\big(\rho\bar{\rho}\mu_r^2\big). \tag{17}$$

In arriving at Eq. (17) we have used the asymptotic form $K_1(Q'\rho) \propto \exp[-Q'\rho]$ for the Bessel-K functions, anticipating that, for small $\alpha_s(\mu_r)$, the dominant contribution to Eq. (3) will come from the region $Q'\,\rho(\bar{\rho}) \gg 1$. Note that the parameters Δ_1 and Δ_2 allow us to trace the impact of the two-loop improvement of the I-density, with the one-loop expression [2] corresponding to $\Delta_1 = 1$ and $\Delta_2 = 0$. This is to be contrasted with previous related studies which either ignored the crucial renormalization-scale dependences altogether [15,16] or were still too crude for a study of the associated uncertainties [7] (c.f. also Fig. 3 (left) below).

[3] The saddle-point corresponds to the most-attractive $I\bar{I}$-orientation. We have checked [9] that taking into account the *exact* orientation dependence of the valley action [20] gives *numerically* a very similar result.

[4] Some *initial-state* and *initial-state* - final-state corrections might exponentiate as well [23]. These are not taken into account by the valley action.

The corresponding saddle-point in R_μ, ρ and $\bar{\rho}$ is most easily found in the $p'g$ centre-of-mass (c.m.) system. One finds $R_\mu^* = (-i\rho^*\sqrt{\xi^*-2}, \mathbf{0})$ and $\rho^* = \bar{\rho}^*$, where ξ^* and ρ^* are the solutions of the following saddle-point equations,

$$\frac{1}{2}\frac{\sqrt{\frac{1-x'}{x'}}}{\sqrt{\xi^*-2}}\,Q'\rho^* - \left(\frac{4\pi}{\alpha_s(\mu_r)} - 2\,\Delta_1\,\beta_0 \ln(\rho^*\mu_r)\right)\frac{dS^{(I\bar{I})}(\xi_*)}{d\xi^*} = 0\,, \tag{18}$$

$$\left(\frac{1}{2}\sqrt{\frac{1-x'}{x'}}\,\sqrt{\xi^*-2} - 1\right)Q'\rho^* + \Delta_1\,\beta_0 S^{(I\bar{I})}(\xi^*) - \Delta_2 = 0\,. \tag{19}$$

Upon evaluating the integrand in Eq. (3) at the saddle-point and taking into account the integration over the (Gaussian) fluctuations about the saddle-point [5], we may finally express the cross-section entirely in terms of $v^* \equiv Q'\rho^*$ and ξ^*,

$$\begin{aligned} Q'^2\,\sigma_{p'g}^{(I)} = {} & d^2\frac{\sqrt{12}}{2^{16}}\pi^{15/2}\left((\xi^*+2)v^{*2} + 4\tilde{S}(\tilde{S}-2v^*)\right)\left(\frac{(\xi^*-2)}{\xi^*}\frac{\Delta_1\beta_0}{D(\tilde{S})}\right)^{7/2} \\ & \times\omega(\xi^*)^{2n_f-1}\frac{(\xi^*-2)^3 v^{*5}}{(v^*-\tilde{S})^{9/2}\sqrt{(\xi^*+2)v^*-4\tilde{S}}\sqrt{\frac{1}{2}(\tilde{S}-v^*-2D(\tilde{S}))^2 + \tilde{S}(\tilde{S}-v^*)D\left(\ln\left(\frac{D(\tilde{S})}{\sqrt{\xi^*-2}}\right)\right)}} \\ & \times\left(\frac{4\pi}{\alpha_s(\mu_r)}\right)^{19/2}\exp\left[-\frac{4\pi}{\alpha_s(\mu_r)}S^{(I\bar{I})}(\xi^*) - 2\left(1-\ln\left(\frac{v^*\mu_r}{Q'}\right)\right)\tilde{S}\right], \end{aligned}$$

$$Q'^2\,\sigma_{\bar{q}'q}^{(I)} = \frac{32}{3}\,\frac{\alpha_s(\mu_r)}{4\pi}\,\frac{1}{v^*}\,\frac{\sqrt{x'(1-x')}}{\omega(\xi^*)}\,Q'^2\,\sigma_{p'g}^{(I)}\,, \quad \sigma_{q'q}^{(I)} = (1-\delta_{q'q})\sigma_{\bar{q}'q}^{(I)}\,, \tag{20}$$

where we have introduced the shorthands

$$\tilde{S}(\xi^*) \equiv \Delta_1\,\beta_0 S^{(I\bar{I})}(\xi^*) - \Delta_2\,, \quad D(f(\xi^*)) \equiv \frac{d}{d\ln(\xi^*-2)}f(\xi^*)\,. \tag{21}$$

For completeness, we have listed also the corresponding expression for the $\bar{q}'q$ cross-section (21).

What remains is to solve the saddle-point equations, (18) and (19). An *analytical solution* [9] in the asymptotic regime $\alpha_s(Q') \to 0$, x' and μ_r/Q' fixed, confirms our qualitative expectations (10). In particular one finds, asymptotically, $R^*/\rho^* = \sqrt{\xi^*-2} \to 2/\sqrt{1/x'-1}$. However, for experimentally accessible values of the virtuality Q', the corrections to the asymptotic result are quite large and the corresponding analytical expressions complicated. Hence, we only present here the results corresponding to a *numerical* solution of the saddle-point equations.

In Fig. 3, we display the residual renormalization-scale dependencies of the I-subprocess cross-sections (20) and (21) over a *large* range of μ_r/Q'. Apparently, we have achieved great progress in stability and hence predictivity by using the two-loop renormalization-group invariant form of the I-density $D(\rho, \mu_r)$ from Eqs. (4) and (5): The residual dependence on the renormalization scale μ_r turns out to be strongly reduced as compared to the one-loop case ($\Delta_1 = 1, \Delta_2 = 0$).

[5] We have checked that our result for the Gaussian integrations coincides, for the one-loop case ($\triangle_1 = 1, \triangle_2 = 0$), with the corresponding result quoted in Ref. [16].

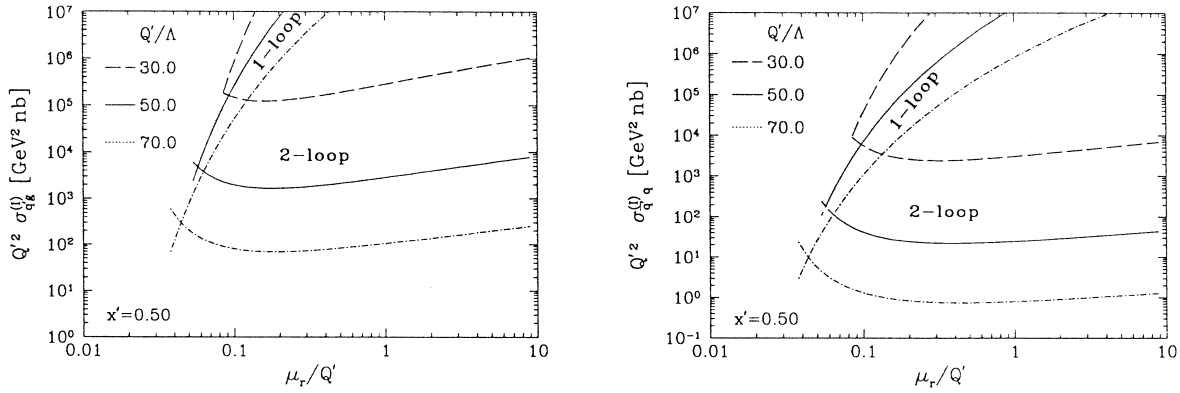

Fig. 3. Renormalization-scale dependences of the I-subprocess cross-sections for a target gluon, Eq. (20), (left) and a target quark, Eq. (21), both for $n_f = 3$.

Intuitively one may expect [4,16,3] $\mu_r \sim 1/\langle \rho \rangle \sim Q'/\beta_0 = \mathcal{O}(0.1)\, Q'$. Indeed, this guess turns out to match quite well our actual choice of the ''best'' scale, $\mu_r = 0.15\, Q'$, for which $\partial \sigma^{(I)}_{q'g}/\partial \mu_r \simeq 0$ (c.f. Fig. 3 (left)). We also note that the cross-sections for a target gluon (Fig. 3 (left)) are about two orders of magnitudes larger than the cross-sections for a target quark (Fig. 3 (right)). Henceforth, the latter are neglected.

Our quantitative results on $\sigma^{(I)}_{q'g}$ are shown in detail in Fig. 4, both as functions of Q'^2 (left) and of x' (right). The dotted curves indicating lines of constant ρ^* (left) and of constant R^*/ρ^* (right) nicely illustrate the qualitative relations (10): For growing Q'^2 and fixed x', smaller and smaller instantons, $\rho^* \sim 1/Q'$, are probed and the cross-sections decrease rapidly, mainly because of the large powers of ρ in the I-density (4). For decreasing x' and fixed Q'^2, on the other hand, the $I\bar{I}$-separation R^* in units of the I-size ρ^* decreases and the cross-section increases dramatically. In the language of the $I\bar{I}$-valley method the latter originates mainly from the attractive interaction between instantons and anti-instantons.

3. We have seen that the collective coordinate integrals in (3) are dominated by a single, calculable saddle-point $(\rho^*, R^*/\rho^*)$, in one-to-one relation to the conjugate momentum variables (Q', x'). This effective one-to-one mapping of the conjugate I-variables allows for the following important strategy: We may determine

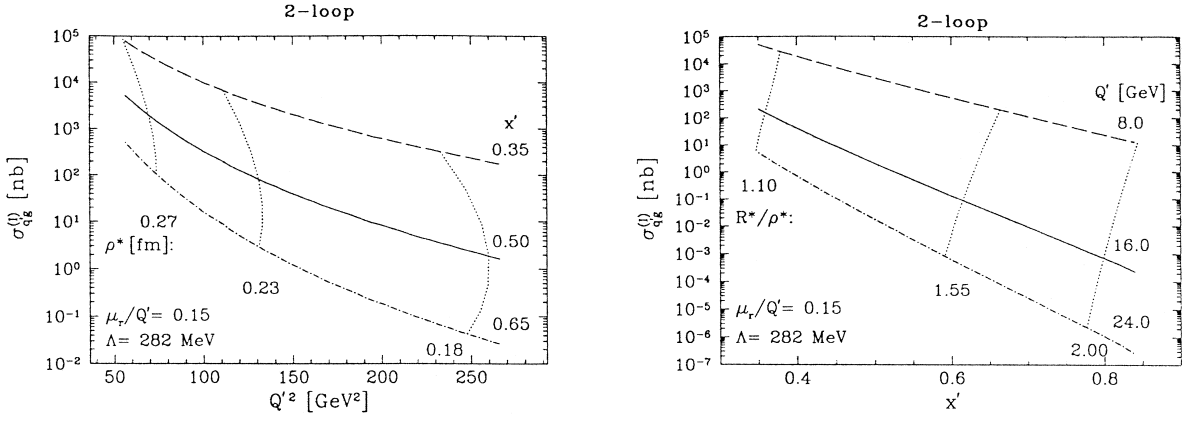

Fig. 4. The instanton-subprocess cross-section (20), for $n_f = 3$, both as functions of Q'^2 (left) and x' (right). The dotted curves are lines of constant I-size ρ^* (left) and of constant $I\bar{I}$-separation R^* in units of the I-size ρ^* (right).

quantitatively the range of validity of I-perturbation theory and the dilute I-gas approximation in the instanton collective coordinates ($\rho \leq \rho_{\max}, R/\rho \geq (R/\rho)_{\min}$) from recent (non-perturbative) lattice simulations of QCD and translate the resulting constraints via the mentioned one-to-one relations into a ''fiducial'' kinematical region ($Q' \geq Q'_{\min}, x' \geq x'_{\min}$).

In lattice simulations 4d-Euclidean space-time is made discrete; specifically, the ''data'' from the UKQCD collaboration [24], which we shall use here, involve a lattice spacing $a = 0.055 - 0.1$ fm and a volume $V = l_{\text{space}}^3 \cdot l_{\text{time}} = [16^3 \cdot 48 - 32^3 \cdot 64]\, a^4$. In principle, such a lattice allows to study the properties of an ensemble of (anti-)instantons with sizes $a < \rho < V^{1/4}$. However, in order to make instanton effects visible, a certain ''cooling'' procedure has to be applied first. It is designed to filter out (dominating) fluctuations of *short* wavelength $\mathcal{O}(a)$, while affecting the topological fluctuations of much longer wavelength $\rho \gg a$ comparatively little. For a discussion of lattice-specific caveats, like possible lattice artefacts and the dependence of results on ''cooling'' etc., see Refs. [11,24].

The first important quantity of interest, entering I-induced cross-sections (c.f. Eq. (3)), is the *I-density* $D(\rho)$, Eq. (4). This power law, $D(\rho)_{|\, n_f = 0} \propto \rho^6$, of I-perturbation theory is confronted in Fig. 5(left) with recent lattice ''data'', which strongly suggests semi-classical I-perturbation theory to be valid for $\rho \lesssim \rho_{\max} \simeq 0.3$ fm. Next, consider the square of the total topological charge, $Q^2 = (n - \bar{n})^2$, along with the total number of charges, $N_{\text{tot}} = n + \bar{n}$. For a *dilute gas*, the number fluctuations are *poissonian* and correlations among the n and $\bar{n}$ distributions absent, implying $\langle Q^2/N_{\text{tot}} \rangle = 1$. From Fig. 5(right), it is apparent that this relation, characterizing the validity of the dilute I-gas approximation, is well satisfied for sufficiently *small* instantons. Again, we find $\rho_{\max} \simeq 0.3$ fm, quite independent of the number of cooling sweeps. For increasing $\rho_{\max} \gtrsim 0.3$ fm, the ratio $\langle Q^2/N_{\text{tot}} \rangle$ rapidly and strongly deviates from one.

Crucial information about a second quantity of interest, the *$I\bar{I}$-interaction*, may be obtained as well from the lattice [11,24]. Quite generally, it is found that the semi-classical attraction for large $R^2/(\rho\bar{\rho})$ turns into a non-perturbative repulsion for smaller separations in units of the sizes, such that in vacuum [6] $\langle R^2/(\rho\bar{\rho}) \rangle = \mathcal{O}(1)$. Thus it seems a reasonable extrapolation to use the attractive, semi-classical valley result for the $I\bar{I}$-interaction Ω, Eq. (11), down to a minimum conformal separation $\xi_{\min} \simeq 3$, corresponding to $(R^*/\rho^*)_{\min} \simeq 1$.

Finally, by means of the discussed saddle-point translation, these lattice constraints may be turned into a ''fiducial'' kinematical region for our cross-section predictions in DIS (c.f. Fig. 4),

$$\left.\begin{array}{lcll} \rho^* & \leq & \rho^*_{\max} & \simeq 0.3\,\text{fm}; \\ \dfrac{R^*}{\rho^*} & \geq & \left(\dfrac{R^*}{\rho^*}\right)_{\min} & \simeq 1 \end{array}\right\} \Rightarrow \left\{\begin{array}{lcll} Q' & \geq & Q'_{\min} & \simeq 8\,\text{GeV}; \\ x' & \geq & x'_{\min} & \simeq 0.35. \end{array}\right. \tag{22}$$

Unlike DIS, where only *small* instantons are probed, in the I-liquid model of Ref. [27] more emphasis is placed on the physics associated with *larger* instantons. For I-ensembles including also larger I-sizes $\gtrsim 0.3$ fm, the various recent lattice results [11,24–26] do not, however, unanimously support the liquid picture.

4. Experimentally, in deep inelastic eP scattering at HERA, the cuts (23) must be implemented via a (Q', x') reconstruction from the final-state momenta and topology [8], while theoretically, they are incorporated into our I-event generator [6] ''QCDINS 1.6.0'' and the resulting prediction of the I-induced cross-section in DIS at

[6] Published ratios range from $\langle R \rangle / \langle \rho \rangle \simeq 0.83$ [24], $\langle R/(\rho + \bar{\rho}) \rangle \simeq 0.59$ [25] to $\langle R/(\rho + \bar{\rho}) \rangle \simeq 1$ [26].

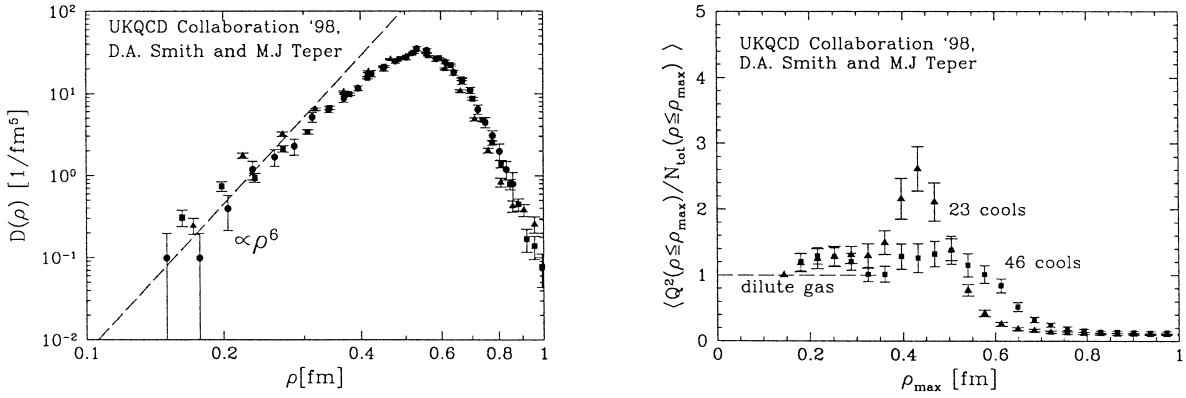

Fig. 5. Support for the validity of I-perturbation theory for the I-density $D(\rho)$ (left) and the dilute I-gas approximation (right) for $\rho < \rho_{\max} \simeq 0.3$ fm from recent lattice data [24].

HERA. The latter is connected to the I-subprocess cross-sections $\sigma^{(I)}_{p'p}$ by the differential $p'p$ luminosity [9] (c.f. Eq. (2)),

$$\frac{d\mathscr{L}^{(I)}_{p'p}}{dx'\,dQ'^2} = \frac{2\pi\alpha^2}{S}\frac{e^2_{p'}}{x'^2}\int_{x_{\mathrm{Bj}\,\min}}^{x'}\frac{dx}{x}\int_{x_{\mathrm{Bj}\,\min}}^{x}\frac{dx_{\mathrm{Bj}}}{x_{\mathrm{Bj}}}\int_{y_{\mathrm{Bj}\,\min}}^{y_{\mathrm{Bj}\,\max}}\frac{dy_{\mathrm{Bj}}}{y_{\mathrm{Bj}}}\,P_{\gamma^*}(y_{\mathrm{Bj}})\,P^{(I)}_{p'}\left(\frac{x}{x'},\dots\right)f_p\left(\frac{x_{\mathrm{Bj}}}{x},\dots\right). \tag{23}$$

Here $S(\simeq 9\times 10^4\,\mathrm{GeV}^2$ for HERA) denotes the c.m. energy squared of the eP collision, $e^2_{p'}$ is the electric charge squared of the current (anti-)quark in units of the electric charge squared, $e^2 = 4\pi\alpha$, and P_{γ^*} denotes the familiar Weizsäcker-Williams-type photon flux,

$$P_{\gamma^*}(y_{\mathrm{Bj}}) = \left(1+(1-y_{\mathrm{Bj}})^2\right)/y_{\mathrm{Bj}}, \tag{24}$$

with $y_{\mathrm{Bj}} = Q^2/(Sx_{\mathrm{Bj}})$. Furthermore, $f_p(x_{\mathrm{Bj}}/x,\dots)$ denotes the density of the target parton p in the proton, with the dots standing for the factorization scale, and, finally, the factor $P^{(I)}_{p'}$ accounts for the flux of virtual (anti-)quarks p' in the I-background entering the I-induced $p'p$-subprocess from the photon side [7,9] (c.f. Fig. 1),

$$P^{(I)}_{q'}\left(\frac{x}{x'},x,\frac{Q'}{Q}\right) \equiv P^{(I)}_{\bar{q}'}\left(\frac{x}{x'},x,\frac{Q'}{Q}\right) \simeq \frac{3}{16\pi^3}\frac{x}{x'}\left(1+\frac{1}{x}-\frac{1}{x'}-\frac{Q'^2}{Q^2}\right). \tag{25}$$

The I-induced cross-section in DIS at HERA, $\sigma^{(I)}_{\mathrm{HERA}}$, subject to kinematical cuts ($x_{\mathrm{Bj}} \geq x_{\mathrm{Bj}\,\min}$; $y_{\mathrm{Bj}\,\max} \geq y_{\mathrm{Bj}} \geq y_{\mathrm{Bj}\,\min}$; $x' \geq x'_{\min}$; $Q' \geq Q'_{\min}$), is then obtained by integrating Eq. (2) over the appropriate range of x' and Q'^2.

Let us point out that the factorization of the eP cross-section for fixed x' and Q'^2 into a sum of differential luminosities and I-subprocess cross-sections, is essential for the possibility to place *different cuts* on the Bjorken variables of the eP and the $p'p$ system, respectively. Of particular interest is $x_{\mathrm{Bj}\,\min} \ll x'_{\min}$. Such cuts permit to explore essentially the full accessible (x_{Bj},x,Q^2) range in DIS at HERA, down to $(10^{-3},10^{-3},10\ \mathrm{GeV}^2)$, say. By placing in this region the additional cuts (23) on (x',Q'^2), I-searches benefit from the high statistics at small x_{Bj}, while the theoretical control is retained over the I-dynamics.

In Ref. [3], on the other hand, (only) the *infrared safe* pieces of the I-induced contributions to the parton-structure functions, $\mathscr{F}^{(I)}_{2\,p}(x,Q^2)$, were estimated in one step by means of configuration space techniques. In our momentum space language, the authors have implicitly *integrated* over Q'^2 and x', with $x_{\mathrm{Bj}} \leq x \leq x' \leq 1$. Hence, the results of Ref. [3] can only be applied [5] to relatively large $x_{\mathrm{Bj}\,\min} = x'_{\min} \sim 0.35$.

Nevertheless, as an important check of our calculations, we have also calculated the *infrared-safe*, *I*-induced contributions to the parton-structure functions, by integrating our asymptotic results over x' and Q'^2 and retaining only the contributions from the upper Q'^2-integration limit $\propto Q^2$. Within the common range of validity [9] of various employed approximations, we find perfect agreement with the gluon-structure function quoted in Ref. [3].

Fig. 6 displays the finalized *I*-induced cross-section at HERA, as function of the cuts $x'_{\min}$ and $Q'_{\min}$, as obtained with the new release ''QCDINS 1.6.0'' of our *I*-event generator. Only the target gluon contribution has been taken into account. For the minimal cuts (23) extracted from lattice simulations, we specifically obtain

$$\sigma^{(I)}_{\rm HERA}(x' \geq 0.35, Q' \geq 8\,{\rm GeV}) \simeq 126\,{\rm pb}; \quad \text{for } x_{\rm Bj} \geq 10^{-3}; 0.9 \geq y_{\rm Bj} \geq 0.1. \tag{26}$$

Hence, with the total luminosity accumulated by experiments at HERA, $\mathscr{L} = \mathscr{O}(80)\ {\rm pb}^{-1}$, there should be already $\mathscr{O}(10^4)$ *I*-induced events from this kinematical region on tape. Note also that the cross-section quoted in Eq. (27) corresponds to a fraction of *I*-induced to normal DIS (nDIS) events of

$$f^{(I)} = \frac{\sigma^{(I)}_{\rm HERA}}{\sigma^{(\rm nDIS)}_{\rm HERA}} = \mathscr{O}(1)\,\%; \quad \text{for } x_{\rm Bj} \geq 10^{-3}; 0.9 \geq y_{\rm Bj} \geq 0.1. \tag{27}$$

This is remarkably close to the published upper limits on the fraction of *I*-induced events [29], which are also on the one percent level.

There are still a number of significant uncertainties in our cross-section estimate. For *fixed Q′- and x′-cuts*, one of the dominant uncertainties arises from the experimental uncertainty in the QCD scale Λ. We used in the two-loop expression for α_s with $n_f = 3$ massless flavours the value $\Lambda^{(3)}_{\overline{\rm MS}} = 282$ MeV, corresponding to the central value of the DIS average for $n_f = 4$, $\Lambda^{(4)}_{\overline{\rm MS}} = 234$ MeV [28]. If we change $\Lambda^{(3)}_{\overline{\rm MS}}$ within the allowed range, $\approx \pm 65$ MeV, the cross-section (27) varies between 26 pb and 426 pb. Minor uncertainties are associated with the residual renormalization-scale dependence (c.f. Fig. 3) and the choice of the factorization scale. Upon varying the latter by an order of magnitude, the changes are in the $\mathscr{O}(20)$ % range.

By far the most dominant uncertainty arises, however, from the unknown boundaries of the fiducial region in (x', Q') (c.f. Fig. 6). Here, the constraints from lattice simulations are extremely valuable for making concrete predictions.

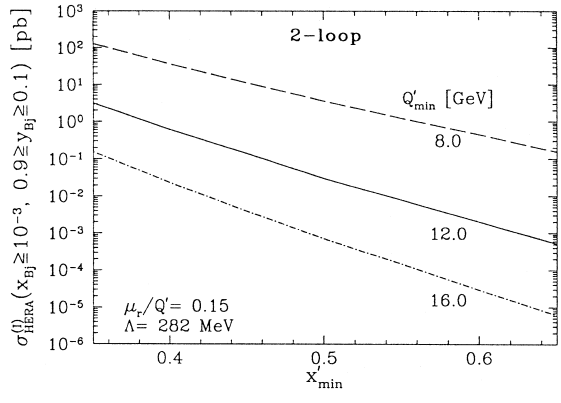

Fig. 6. Instanton-induced cross-section at HERA ($n_f = 3$).

Acknowledgements

We would like to thank S. Moch for valuable contributions in the early stage of this work. We would like to acknowledge helpful discussions with I. Balitsky, V. Braun and N. Kochelev.

References

[1] A. Belavin, A. Polyakov, A. Schwarz, Yu. Tyupkin, Phys. Lett. B 59 (1975) 85.
[2] G. 't Hooft, Phys. Rev. Lett. 37 (1976) 8; Phys. Rev. D 14 (1976) 3432; D 18 (1978) 2199 (E).
[3] I. Balitsky, V. Braun, Phys. Lett. B 314 (1993) 237.
[4] S. Moch, A. Ringwald, F. Schrempp, Nucl. Phys. B 507 (1997) 134.
[5] A. Ringwald, F. Schrempp, hep-ph/9411217, in: D. Gigoriev et al. (Eds.), Quarks '94, Proc. 8th Int. Seminar, Vladimir, Russia, May 11–18, 1994, pp. 170–193.
[6] M. Gibbs, A. Ringwald, F. Schrempp, hep-ph/9506392, in: J.-F. Laporte, Y. Sirois (Eds.), Proc. Workshop on Deep Inelastic Scattering and QCD Paris, France, April 24–28, 1995, pp. 341–344.
[7] A. Ringwald, F. Schrempp, hep-ph/9610213, in: V. Matveev, A. Penin, V. Rubakov, A. Tavkhelidze (Eds.), Quarks '96, Proc. 9th Int. Seminar, Yaroslavl, Russia, May 5–11, 1996, vol. I, pp. 29–54.
[8] T. Carli, A. Ringwald, F. Schrempp, in preparation.
[9] S. Moch, A. Ringwald, F. Schrempp, in preparation.
[10] T. Morris, D. Ross, C. Sachrajda, Nucl. Phys. B 255 (1985) 115.
[11] For a recent review, see: P. van Baal, hep-lat/9709066, Review at Lattice '97, Edinburgh.
[12] C. Bernard, Phys. Rev. D 19 (1979) 3013.
[13] A. Hasenfratz, P. Hasenfratz, Nucl. Phys. B 193 (1981) 210; M. Lüscher, Nucl. Phys. B 205 (1982) 483; G. 't Hooft, Phys. Rev. 142 (1986) 357.
[14] I. Balitsky, hep-ph/9405335, in: A. Smilga (Ed.), Continuous advances in QCD, Proc., Minneapolis, USA, February 18–20, 1994, pp. 167–194.
[15] V.V. Khoze, A. Ringwald, Phys. Lett. B 259 (1991) 106.
[16] I. Balitsky, V. Braun, Phys. Rev. D 47 (1993) 1879.
[17] P. Arnold, M. Mattis, Phys. Rev. D 44 (1991) 3650; A. Mueller, Nucl. Phys. B 364 (1991) 109; D. Diakonov, V. Petrov, in: Proc. of the 26th LNPI Winter School (Leningrad, 1991), pp. 8–64.
[18] M. Porrati, Nucl. Phys. B 347 (1990) 371; V.V. Khoze, A. Ringwald, Nucl. Phys. B 355 (1991) 351; V. Zakharov, Nucl. Phys. B 371 (1992) 637; I. Balitsky, V. Braun, Nucl. Phys. B 380 (1992) 51.
[19] A. Yung, Nucl. Phys. B 297 (1988) 47.
[20] J. Verbaarschot, Nucl. Phys. B 362 (1991) 33.
[21] E. Shuryak, J. Verbaarschot, Phys. Rev. Lett. 68 (1992) 2576.
[22] C. Callan, R. Dashen, D. Gross, Phys. Rev. D 17 (1978) 2717.
[23] A. Mueller, Nucl. Phys. B 348 (1991) 310; B 353 (1991) 44.
[24] D. Smith, M. Teper, Edinburgh preprint 98-1, hep-lat/9801008.
[25] P. de Forcrand, M. Pérez, I. Stamatescu, Nucl. Phys. B 499 (1997) 409.
[26] T. DeGrand, A. Hasenfratz, T. Kovács, Nucl. Phys. B 505 (1997) 417.
[27] E.V. Shuryak, Nucl. Phys. B 198 (1982) 83; T. Schäfer, E.V. Shuryak, Rev. Mod. Phys. 70 (1998) 323.
[28] Review of Particle Physics, Particle Data Group, Phys. Rev. D 54 (1996) 1.
[29] S. Aid et al., H1 Collaboration, Nucl. Phys. B 480 (1996) 3; S. Aid et al., H1 Collaboration, Z. Phys. C 72 (1996) 573; T. Carli, M. Kuhlen, Nucl. Phys. B 511 (1998) 85.